Whole-exome sequencing identifies tetratricopeptide repeat domain 7A (*TTC7A*) mutations for combined immunodeficiency with intestinal atresias

Rui Chen, PhD,[a]* Silvia Giliani, PhD,[b]* Gaetana Lanzi, PhD,[b] George I. Mias, PhD,[a] Silvia Lonardi, BS,[c] Kerry Dobbs, BS,[d] John Manis, MD,[e] Hogune Im, PhD,[a] Jennifer E. Gallagher, PhD,[a]‡ Douglas H. Phanstiel, PhD,[a] Ghia Euskirchen, PhD,[a] Philippe Lacroute, PhD,[a] Keith Bettinger, MS,[a] Daniele Moratto, PhD,[b] Katja Weinacht, MD,[f] Davide Montin, MD,[g] Eleonora Gallo, MD,[g] Giovanna Mangili, MD,[h] Fulvio Porta, MD,[i] Lucia D. Notarangelo, MD,[i] Stefania Pedretti, MD,[h] Waleed Al-Herz, MD,[j] Wasmi Alfahdli, MD,[k] Anne Marie Comeau, PhD,[l] Russell S. Traister, MD, PhD,[m] Sung-Yun Pai, MD,[n] Graziella Carella, PhD,[o] Fabio Facchetti, MD,[c] Kari C. Nadeau, MD, PhD,[p] Michael Snyder, PhD,[a] and Luigi D. Notarangelo, MD[d,q] *Stanford, Calif, Brescia, Torino, and Bergamo, Italy, Boston and Worcester, Mass, Kuwait City, Kuwait, and Pittsburgh, Pa*

Background: Combined immunodeficiency with multiple intestinal atresias (CID-MIA) is a rare hereditary disease characterized by intestinal obstructions and profound immune defects.

Objective: We sought to determine the underlying genetic causes of CID-MIA by analyzing the exomic sequences of 5 patients and their healthy direct relatives from 5 unrelated families.

Methods: We performed whole-exome sequencing on 5 patients with CID-MIA and 10 healthy direct family members belonging to 5 unrelated families with CID-MIA. We also performed targeted Sanger sequencing for the candidate gene tetratricopeptide repeat domain 7A (*TTC7A*) on 3 additional patients with CID-MIA.

Results: Through analysis and comparison of the exomic sequence of the subjects from these 5 families, we identified biallelic damaging mutations in the *TTC7A* gene, for a total of 7 distinct mutations. Targeted *TTC7A* gene sequencing in 3 additional unrelated patients with CID-MIA revealed biallelic deleterious mutations in 2 of them, as well as an aberrant splice product in the third patient. Staining of normal thymus showed that the TTC7A protein is expressed in thymic epithelial cells, as well as in thymocytes. Moreover, severe lymphoid depletion was observed in the thymus and peripheral lymphoid tissues from 2 patients with CID-MIA.

Conclusions: We identified deleterious mutations of the *TTC7A* gene in 8 unrelated patients with CID-MIA and demonstrated that the TTC7A protein is expressed in the thymus. Our results strongly suggest that *TTC7A* gene defects cause CID-MIA. (J Allergy Clin Immunol 2013;132:656-64.)

Key words: *Combined immunodeficiency with multiple intestinal atresias, tetratricopeptide repeat domain 7A, whole-exome sequencing, thymus*

From the Departments of [a]Genetics and [p]Pediatrics, Stanford University School of Medicine; [b]A. Nocivelli Institute for Molecular Medicine, Pediatric Clinic, University of Brescia, and the Section of Genetics, Department of Pathology Spedali Civili, Brescia; [c]the Department of Pathology, University of Brescia; [d]the Division of Immunology, Boston Children's Hospital, Harvard Medical School, Harvard Stem Cell Institute, Boston; [e]the Department of Transfusion Medicine, [f]the Division of Hematology and Oncology, and [n]the Division of Hematology-Oncology, Boston Children's Hospital; [g]the Department of Public Health and Pediatrics, University of Torino; [h]USC Patologia Neonatale, Ospedali Riuniti di Bergamo; [i]the Division of Pediatric Hematology-Oncology and [o]Clinical Immunology and Allergology, Spedali Civili Brescia; [j]the Department of Pediatrics, Al-Sabah Hospital, Kuwait City; [k]the Department of Surgery, Ibn-Sina Hospital, Kuwait City; [l]the New England Newborn Screening Program, University of Massachusetts Medical School, Worcester; [m]the Department of Internal Medicine, Children's Hospital of Pittsburgh; and [q]Harvard Stem Cell Institute, Harvard Medical School, Boston.

*These authors contributed equally to this work.

‡Dr Gallagher is currently affiliated with the Department of Biology, West Virginia University, Morgantown, WV.

M.S. is funded by grants from Stanford University and the National Institutes of Health (NIH). L.D.N. is supported by NIH grants 5P01AI076210-04, 1R01AI00887-01, and 4U54AI082973-04 (also to S.-Y.P.) and the Manton Foundation. Both L.D.N. and W.A.-H. are supported by a grant from the Dubai Harvard Foundation for Medical Research and by Kuwait Foundation for the Advancement of Sciences (grant 2010-1302-05). S.G. is supported by Fondazione Nocivelli and the University of Brescia. F.F. is supported by MIUR (grant 20104HBZ8E_002). S.-Y.P. is supported by a Translational Investigator Service award from Boston Children's Hospital. G.I.M.'s research reported in this publication was supported by the National Human Genome Research Institute of the NIH under award no. K99HG007065. The content is solely the responsibility of the authors and does not necessarily represent the official views of the NIH. D.H.P. is a Damon Runyon Fellow supported by the Damon Runyon Cancer Research Foundation (DRG-#2122-22).

Disclosure of potential conflict of interest: G. I. Mias has received grants from the National Institutes of Health (NIH) and the National Genome Research Institute. S. Lonardi is employed by the University of Brescia. J. Manis has received grants from NIH. G. Euskirchen receives part of her salary from NIH grants. S.-Y. Pai has received grants from NIH/National Institute of Allergy and Infectious Diseases (NIAID), has received a Translational Investigator Service internal award from Boston Children's Hospital, and has grants/grants pending from the Manton Foundation, NIH/NIAID, and NIH/National Heart, Lung, and Blood Institute (NHLBI). F. Facchetti has received the Bruto salary from the University of Brescia and has grants/grants pending from the Italian Ministry of University and Research. M. Snyder is a scientific advisory board member for Personalis and Genapsys; has consultant arrangements with Illumina; has received payment for lectures, including service on speakers' bureaus, from Illumina and Beckman Coulter; and has stock/stock options in Excelexis. L. D. Notarangelo has received grants from the NIH and the Dubai Harvard Foundation for Medical Research, is a board member for the Immune Disease Institute, is an advisory board member for Meyer Hospital, is employed by Boston Children's Hospital, and receives royalties from UpToDate. The rest of the authors declare that they have no relevant conflicts of interest.

Received for publication May 23, 2013; revised June 16, 2013; accepted for publication June 18, 2013.

Available online July 4, 2013.

Corresponding author: Michael Snyder, PhD, Department of Genetics, Stanford University School of Medicine, Stanford, CA 94305. E-mail: mpsnyder@stanford.edu. Or: Kari C. Nadeau, MD, PhD, Department of Pediatrics, Stanford University, Stanford, CA 94305. E-mail: knadeau@stanford.edu. Or: Luigi D. Notarangelo, MD, Division of Immunology, Boston Children's Hospital, Harvard Medical School, Harvard Stem Cell Institute, Boston, MA 02115. E-mail: Luigi.Notarangelo@childrens.harvard.edu.

0091-6749/$36.00

http://dx.doi.org/10.1016/j.jaci.2013.06.013

Abbreviations used

CID-MIA:	Combined immunodeficiency with multiple intestinal atresias
GATK:	Genome Analysis Toolkit
GvHD:	Graft-versus-host disease
HCT:	Hematopoietic cell transplantation
Indels:	Insertions and/or deletions
NMD:	Nonsense-mediated decay
SCID:	Severe combined immunodeficiency
SNV:	Single nucleotide variant
TREC:	T-cell receptor excision circle
TTC7A:	Tetratricopeptide repeat domain 7A
WES:	Whole-exome sequencing

Hereditary multiple intestinal atresias (MIA; OMIM 243150) is a rare condition characterized by a variable number of atresias that might affect both the small and the large bowel.[1,2] The disease is typically very severe, requiring early surgical intervention. The association of MIA with immunodeficiency was reported for the first time in 1990[3] and confirmed by several additional studies.[4-7] Severe combined immunodeficiency (SCID), leading to increased susceptibility to bacterial and opportunistic infections,[4-7] and fatal graft-versus-host disease (GvHD) after transfusion of unirradiated blood products or combined liver and small bowel transplantation have been reported.[8,9]

Although most cases of combined immunodeficiency with multiple intestinal atresias (CID-MIA) are sporadic, a genetic basis with autosomal recessive inheritance was postulated when 5 French-Canadian cases in 3 sibships with common ancestry were described.[10] Recurrence of cases in the same sibship[3,6,7,11,12] and parental consanguinity[5,11,13-15] have since been reported in several other families of various descent.

Whole-exome sequencing (WES) is a powerful tool for studies of hereditary diseases in which obvious gene candidates have been ruled out.[16-18] By using WES, we have identified deleterious biallelic mutations in the tetratricopeptide repeat domain 7A (*TTC7A*) gene in 5 patients from unrelated families with SCID-MIA, belonging to different ethnic groups. We have also identified *TTC7A* mutations in 3 additional patients from whom pathologic specimens were available. Staining of normal human thymus by means of immunohistochemistry revealed expression of the TTC7A protein in normal thymus. Severe lymphoid depletion was demonstrated on postmortem examination of the thymus and peripheral lymphoid tissue of 2 of the affected patients. Overall, our results strongly indicate that *TTC7A* mutations are responsible for CID-MIA and interfere with normal thymopoiesis.

METHODS

Human sample collection and DNA extraction

Patients with SCID-MIA and their direct family members were enrolled in our study after obtaining informed consent under institutional review board–approved protocol 04-09-113 (Children's Hospital Boston) and ethics committee approval (Spedali Civili Brescia, Brescia, Italy). Genomic DNA was isolated with the automatic DNA extractor Maxwell 16 (Promega, Madison, Wis).

WES and data analysis

Whole-exome enrichment was performed with the Agilent SureSelect Human All Exon Kit 50M (Agilent Technologies, Santa Clara, Calif) and sequenced with the Illumina HiSeq 2000 sequencer (Illumina, San Diego, Calif). Sequencing reads were mapped with Burrows-Wheeler Aligner (version 0.6.0),[19] and variants were called with the Genome Analysis Toolkit (GATK; version 1.3-17-gc62082b).[20,21] Details are described in the Methods section in this article's Online Repository at www.jacionline.org.

Sanger sequencing validation

The chromosomal regions containing the identified *TTC7A* damaging variants in families F1, F2, F3, F4, and F5 were amplified by means of PCR with the Phusion DNA Polymerase (New England BioLabs, Ipswich, Mass) and subjected to Sanger sequencing through ELIM BIOPHARM (http://www.elimbio.com/). A list of sequencing primers used is included in Table E1 in this article's Online Repository at www.jacionline.org. Sequencing of genomic DNA corresponding to the coding regions of the *TTC7A* (ENST00000319190) gene was performed in patient F6-A and his mother, patients F7-A and F8-A, and parents and siblings of patients F2-A and F3-A by using direct sequencing after PCR amplification of exons and flanking intronic regions. Primers and conditions are available on request.

RNA analysis of human samples

Total RNA was isolated from PBMCs, fibroblasts, and induced pluripotent stem cells by using the RNeasy Mini kit (Qiagen, Hilden, Germany), and 200 ng of DNase I–treated total RNA was transcribed into first-strand cDNA by using the GeneAmp RNA PCR kit (Applied Biosystems, Foster City, Calif). Analysis of *TTC7A* and glyceraldehyde-3-phosphate dehydrogenase (*GAPDH*; as expression control) expression was performed by using real-time PCR with Assays-on-Demand products and TaqMan Master Mix from Applied Biosystems. Primers for RT-PCR are reported in the Methods section in this article's Online Repository.

Immunohistochemistry analysis of TTC7A expression in human tissues

Four-micrometer sections were obtained from formalin-fixed, paraffin-embedded normal human thymus; a mesenteric lymph node biopsy specimen from patient F7-A; and postmortem paraffin-embedded thymus, inguinal lymph node, and spleen tissue from patient F8-A. Details on immunohistochemistry staining are described in the Methods section in this article's Online Repository.

Microarray analysis of murine *Ttc7* mRNA expression

Microarray analysis of *Ttc7* mRNA expression in sorted murine lymphoid cells and in mouse bone marrow thymus were performed, as previously described.[22] Details are provided in the Methods section in this article's Online Repository.

RESULTS

Clinical and immunologic features of patients

We analyzed a total of 8 unrelated patients with CID-MIA. Patient 1 (F1-A) was born to consanguineous parents of Arabic origin and was given a diagnosis of pyloric and anal atresias at birth. Surgery was complicated by *Enterococcus faecalis* bacteremia. Immunologic investigations at 15 days of life revealed moderate T-cell lymphopenia, with a marked decrease in $CD8^+$ T-cell numbers, decreased *in vitro* proliferation to PHA, and severe hypogammaglobulinemia (Fig 1, *A*, and Table I). In spite of supportive treatment, the patient died at 3 months of life during an episode of sepsis caused by *Klebsiella* species.

Patient 2 (F2-A) was born to parents of Serbian origin; one elder brother with a diagnosis of anal atresia died in the first

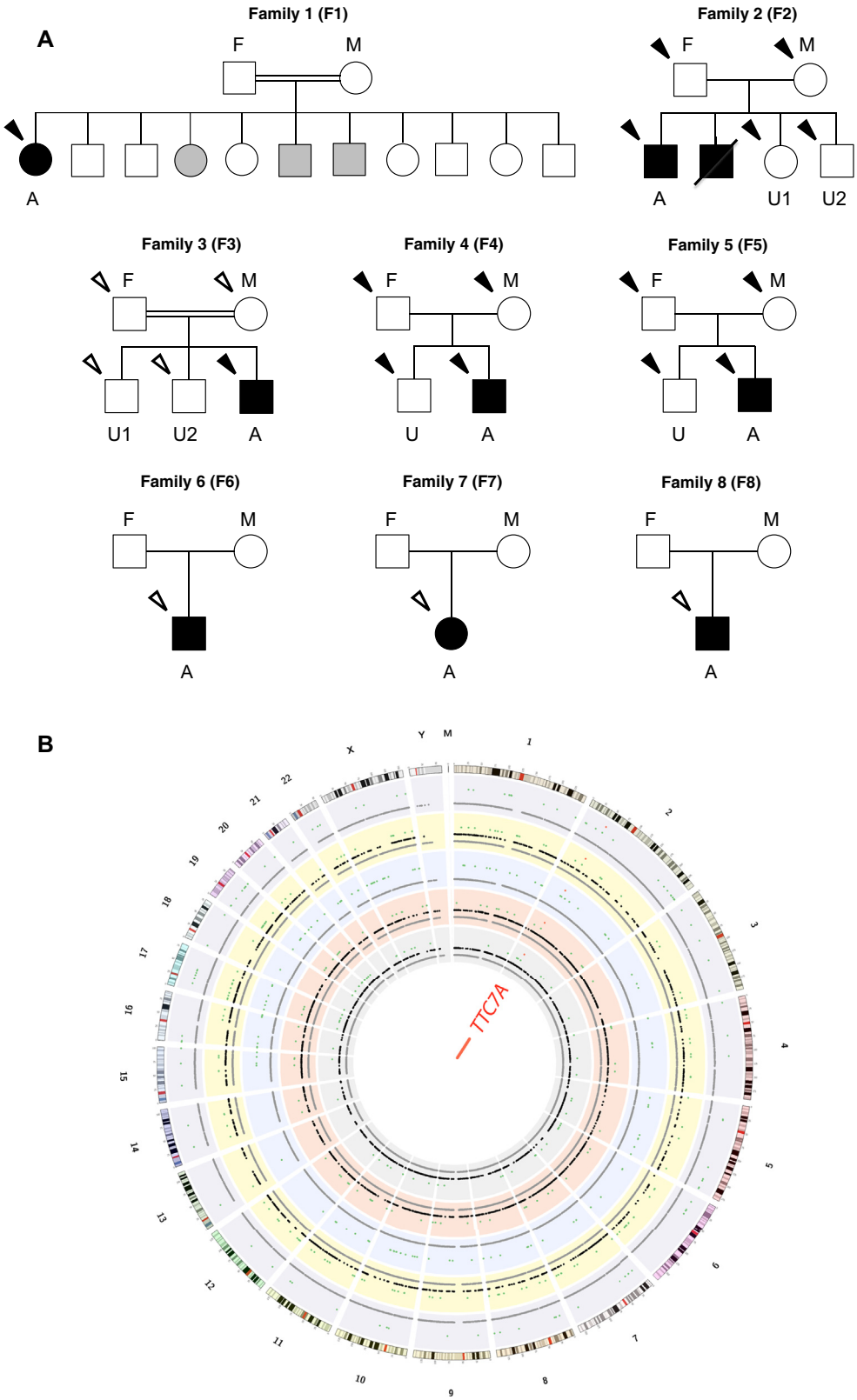

FIG 1. Pedigree of families with CID-MIA and summary of WES. **A,** Pedigree of the 8 families with CID-MIA. *A*, Affected proband; *U*, unaffected offspring; *F*, father; *M*, mother. **B,** Summary of WES results. *Gray dots*, All variants; *black dots*, variants following certain modes of inheritance; *green dots*, potentially damaging variants; *red dots*, mutations in *TTC7A*. The plot was made with Circos.[41]

TABLE I. Immunologic and molecular features of patients with CID-MIA

Parameter	Pt 1 (15 d)	Pt 2 (4 mo)	Pt 3 (10 mo)	Pt 4 (2 y)	Pt 5 (2.5 mo)	Pt 6 (4 mo)	Pt 7 (4 mo)	Pt 8 (10 mo)	Healthy control subjects (normal range)
Sample ID	F1-A	F2-A	F3-A	F4-A	F5-A	F6-A	F7-A	F8-A	
ALC (cells/μL)	3290	1224	620	200	1220	415	260	1269	3400-9000
$CD3^+$ (cells/μL)	1328	338	169	71	74	178	128	824	1900-5900
$CD4^+$ (cells/μL)	1287	261	135	32	49	124	106	ND	1400-4300
$CD8^+$ (cells/μL)	23	7	17	49	14	4	2	ND	500-1700
$CD19^+$ (cells/μL)	429	17	2	4	458	79	15	200	571-3860
$CD16/56^+$ (cells/μL)	97	878	312	30	118	129	55	0	160-950
RTE ($CD4^+45RA^+31^+$ cells/μL)	849	17	35	7	ND	ND	14	ND	800-5800
TRECs (copies/μL)	ND	ND	ND	ND	0-7	ND	ND	ND	>252
Proliferation to PHA (SI)	13.3	ND*	1	11.5	5.6	32	1	ND	>67
IgG (mg/dL)	84	ND	57	242	<75	<100	180	106	232-1411
IgA (mg/dL)	<6	<6	<6	21	<7	<6	<6	ND	0-83
IgM (mg/dL)	<25	<25	<25	<25	5	<25	27	ND	0-145

Sample naming nomenclature: *Fn*, Family n (n = 1~8); *A*, affected offspring (proband); *U/U1/U2*, unaffected offspring; *F*, father of proband; *M*, mother of proband.
ALC, Absolute lymphocyte count; *ND*, not done; *Pt*, patient; *RTE*, recent thymic emigrants.
*In this patient 3 attempts to obtain the karyotype by culturing PBMCs with PHA failed.

month of life. The proband underwent surgery at birth because of multiple atresias affecting the pylorus, ileum, and colon. During hospitalization, he had 2 episodes of *Staphylococcus* species–induced sepsis. Laboratory investigation disclosed T- and B-cell lymphopenia and undetectable serum IgA and IgM levels (Fig 1, *A*, and Table I). He died at 4 months of age.

Patient 3 (F3-A) was born to related parents of Bosniak origin. He presented at birth with meconium peritonitis associated with multiple ileal atresias and underwent several resections. The clinical course was complicated by multiple episodes of sepsis caused by *Pseudomonas aeruginosa* and *Candida albicans* and by abdominal abscesses caused by *P aeruginosa*. Laboratory investigations at 10 months of age showed severe T- and B-cell lymphopenia, absent proliferation to PHA and anti-CD3, and profound hypogammaglobulinemia (Fig 1, *A*, and Table I). He is alive at 2.8 years of age and receiving total parenteral nutrition.

Patient 4 (F4-A) was born at 35 weeks as part of a fraternal twin gestation. At birth, she was found to have multiple intestinal atresias requiring surgery. She experienced multiple episodes of central line, urinary tract, and G-tube site bacterial infections and fungemia. She also had chicken pox after receiving the varicella vaccine. At 2 years of age, she had extreme lymphopenia, severe impairment of proliferation to PHA, and hypogammaglobulinemia with no protective antibody responses to tetanus, diphtheria, or pneumococcus (Fig 1, *A*, and Table I). She is currently on the small bowel transplant list, receiving parenteral nutrition, intravenous immunoglobulin, and *Pneumocystis jiroveci* prophylaxis with pentamidine.

Patient 5 (F5-A) was born at 37 weeks of gestation to a father of French-Canadian descent and a mother of mixed European descent. He received multiple surgeries and resections for treatment of intestinal atresias that were complicated by *Escherichia coli*–induced sepsis. During universal statewide newborn screening for SCID at birth,[23] he was found to have extremely low levels of T-cell receptor excision circles (TRECs; 17 copies/μL; normal value, ≥252 copies/μL). Immunologic investigations disclosed extreme T-cell lymphopenia, severe impairment of proliferation to PHA, and agammaglobulinemia (Fig 1, *A*, and Table I). At 3 months of age, he received hematopoietic cell transplantation (HCT) from his sibling who was mismatched at the *HLA-A* locus in the graft rejection direction only. Conditioning was with serotherapy (antithymocyte globulin) only, and the posttransplantation course was uncomplicated, with no acute or chronic GvHD. He has had multiple resections of atretic intestine after transplantation and continues to be dependent on parenteral nutrition for a short gut. He is now 22 months after transplantation and has attained robust reconstitution of T-cell immunity (see Table E2 in this article's Online Repository at www.jacionline.org).

Patient 6 (F6-A) was born to nonconsanguineous Italian parents and given a diagnosis at birth of multiple intestinal atresias requiring surgical interventions. Use of total parenteral nutrition resulted in significant liver toxicity. At 4 months of age, chronic diarrhea and failure to thrive prompted immunologic investigations that revealed severe T- and B-cell lymphopenia and agammaglobulinemia (Fig 1, *A*, and Table I). Treatment with intravenous immunoglobulin and antimicrobial prophylaxis with trimethoprim/sulfamethoxazole were started. At 10 months of age, the patient received HCT from a matched unrelated donor. Conditioning included cyclophosphamide and thiotepa. Hematologic reconstitution was achieved at 2 weeks. Clinical course was complicated by acute GvHD affecting the skin. Interstitial pneumonia caused by cytomegalovirus led to death at day +55 after transplantation. No data on posttransplantation chimerism are available.

Patient 7 (F7-A) was born to unrelated parents of Italian origin. She was given a diagnosis of pyloric stenosis and underwent pyloroplasty at 3 days of life. In the following weeks, she experienced multiple episodes of sepsis caused by various bacteria (*Klebsiella* species, *E coli*, and *Staphylococcus aureus*) and *Candida* species. At 4 months of age, failure to thrive, severe T-and B-cell lymphopenia, and hypogammaglobulinemia were demonstrated (Fig 1, *A*, and Table I). At the age of 9 months, severe neurodevelopmental delay was present and associated with lack of visual evoked response. The infant was referred elsewhere for possible combined small bowel transplantation and HCT.

Patient 8 (F8-A) was the first child born to unrelated Italian parents. The mother was seropositive for HIV, and the father was affected by a gastric tumor. HIV DNA PCR testing was performed at 2 weeks of age, and results were negative. Soon after birth, the patient underwent surgery for multiple small bowel atresias. At 7

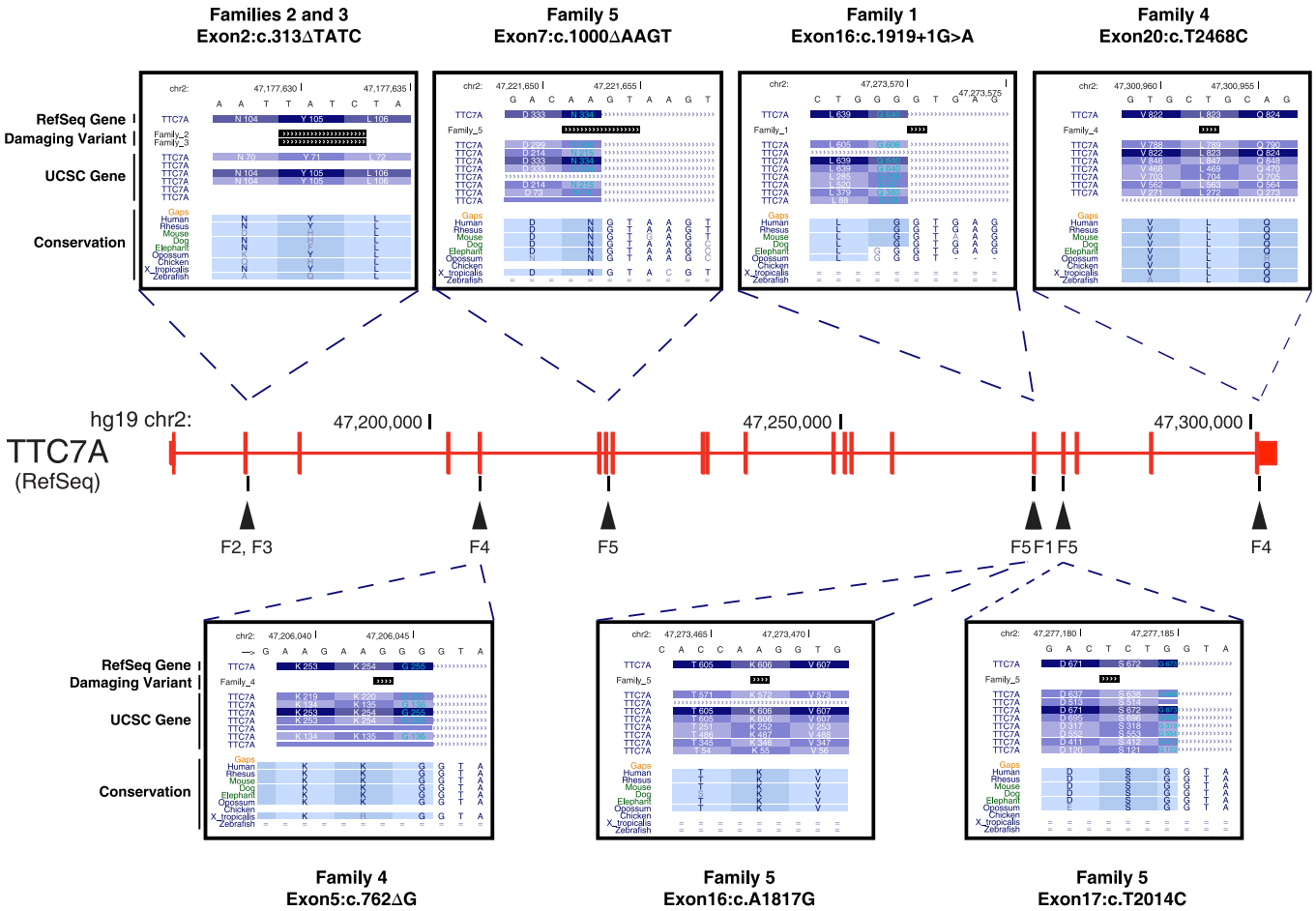

FIG 2. Schematic representation of the *TTC7A* gene and position of the mutations identified in patients with CID-MIA. Exons are identified by *vertical bars*. For each site containing the mutations, from top to bottom, hg19 chromosome location, chromosome sequence, RefSeq gene, damaging variant, UCSC gene, and Vertebrate Multiz Alignment and Conservation are shown. Information was retrieved from the UCSC Genome Browser (http://genome.ucsc.edu/).

months of age, he was referred to our institution with failure to thrive, dyspnea, and hepatosplenomegaly. Laboratory investigations showed lymphopenia affecting T and natural killer cells and hypogammaglobulinemia (Fig 1, *A*, and Table I). During hospitalization, the patient had disseminated *Candida* species infection and died at 8 months of age.

TTC7A mutations were identified in affected probands through WES

We performed WES on 15 subjects (including the 5 probands) from the 5 core families in our study (families 1, 2, 3, 4, and 5; Fig 1).[24] A summary of sequencing statistics is shown in Tables E3 and E4 in this article's Online Repository at www.jacionline.org. From the identified variants (see the Results section and Tables E5 and E6 in this article's Online Repository at www.jacionline.org for details), we screened for variants that followed various potential modes of inheritance for this disease in each of the 5 core families. Of all the potentially damaging variants identified, only those in 1 gene, *TTC7A*, were found in all 5 probands of our core families (Fig 2 and Table II). Patient F1-A harbors a homozygous exon 16 c.1919+1G>A mutation, which is predicted to disrupt the invariant splicing donor site (gt) immediately 3′ to exon 16 and causes read-through into its following intron. Patients F2-A and F3-A both have a homozygous 4-bp deletion (exon 2 c.313ΔTATC), which is predicted to lead to a frameshift mutation at codon 105 (p.Y105fs) and nonsense-mediated decay (NMD) of the resulting RNA transcript. Parents and healthy siblings of patients F2-A and F3-A were all found to be heterozygous carriers of this mutation. Patient F4-A inherited a pair of damaging compound heterozygous mutations (exon 5 c.762ΔG on the maternal allele and exon 20 c.T2468C on the paternal allele), with the former predicted to lead to NMD through a frameshift mutation (p.K254fs) and the latter (p.L823P) predicted to be deleterious by using both the SIFT and PolyPhen-2 tools. Patient F5-A harbored a different combination of compound heterozygous variants (exon 7 c.1000ΔAAGT on the paternal allele, and 2 deleterious single nucleotide variants [SNVs], exon 16 c.A1817G [p.K606R] and exon 17 c.T2014C [p.S672P] on the maternal allele), which were predicted to abolish the function of both alleles. In each case the mutations are not found or rare (<1%) in the 1000 genomes project[25] and Exome Sequencing Project (ESP6500)[26] databases and are located at highly conserved regions of the gene (Fig 2). Four of the 8 deleterious

TABLE II. *TTC7A* mutations identified with WES in the 5 core families with CID-MIA

Families	Chromosome	Position	Damaging variant	rs ID	1-SIFT	PolyPhen-2	SIFT causes NMD
1	2	47273571	Exon16:c.1919+1G>A	–	–	–	–
2	2	47177629	Exon2:c.313ΔTATC	–	–	–	Yes
3	2	47177629	Exon2:c.313ΔTATC	–	–	–	Yes
4	2	47206043	Exon5:c.762ΔG	–	–	–	Yes
4	2	47300953	Exon20:c.T2468C	–	1	0.999	–
5	2	47221651	Exon7:c.1000ΔAAGT	–	–	–	Yes
5	2	47273468	Exon16:c.A1817G	–	1	0.934	–
5	2	47277182	Exon17:c.T2014C	–	0.99	0.984	–

Families	Type	Ref	Alt	A	F	M	U1	U2
1	Recessive SDM	G	A	A/A				
2	Recessive FSD	TTATC	T	T/T	TTATC/T	TTATC/T	TTATC/T	TTATC/T
3	Recessive FSD	TTATC	T	T/T				
4	CH	AG	A	AG/A	AG/AG	AG/A	AG/A	
4	CH	T	C	T/C	T/C	T/T	T/T	
5	CH	CAAGT	C	CAAGT/C	CAAGT/C	CAAGT/CAAGT	CAAGT/C	
5	CH	A	G	A/G	A/A	A/G	A/A	
5	CH	T	C	T/C	T/T	T/C	T/T	

Sample naming nomenclature: *Fn*, Family n (n = 1∼8); *A*, affected offspring (proband); *U/U1/U2*, unaffected offspring; *F*, father of proband; *M*, mother of proband.
Alt, Alternative variant; *CH*, compound heterozygous; *Chr*, chromosome; *FSD*, frameshift deletion; *Ref*, reference sequence; *SDM*, splicing donor mutation.

variants were further confirmed by means of Sanger sequencing in 3 families (F2, F3, and F5; see Fig E1 in this article's Online Repository at www.jacionline.org); the other 4 variants were located in regions that were difficult to amplify because in each case PCR amplification with designed unique primers resulted in multiple bands in 2 attempts (data not shown).

Subsequently, we retrieved biological specimens from patients F6-A, F7-A, and F8-A. Targeted sequencing of the *TTC7A* gene revealed compound heterozygous mutations in patients F6-A (c.C2033A and c.C2134T, leading to p.S678X and p.Q712X premature terminations, respectively) and F7-A (homozygous for the mutation c.T1196C, leading to a p.L399P amino acid change that is predicted to be deleterious by using both the SIFT and PolyPhen-2 tools). For patient F8-A, we did not find any damaging variants using the primers designed for *TTC7A* open reading frame analysis. We then analyzed the cDNA of the *TT7C7A* gene split in 3 portions because of its length. By using a forward primer in exon 1 and a reverse primer in exon 4, both an in-frame cDNA product lacking exons 2 and 3 and a normal-sized cDNA product were detected (see Fig E2 in this article's Online Repository at www.jacionline.org). The genomic mutation causing this aberrant splicing has not been characterized because introns in the region are between 6,000 and 18,000 bp long.

Altered *TTC7A* expression levels in patients with CID-MIA

To check for RNA expression defects, we analyzed *TTC7A* expression by means of quantitative RT-PCR with a TaqMan assay located on the exon 1-2 boundary in 2 patients (F3-A and F5-A) for which we have fibroblasts available. Our analysis showed that relative expression of *TTC7A* in patients F3-A and F5-A compared with that seen in 3 healthy unrelated control subjects was reduced to 32% and 54%, respectively (see Fig E3 in this article's Online Repository at www.jacionline.org). We also performed reverse transcription PCR using RNA from Patient F5-A and found that the exon 7 c.1000ΔAAGT mutation led to skipping of exon 7 (see Fig E4 in this article's Online Repository at www.jacionline.org). Thus the *TTC7A* mutations were shown to affect *TTC7A* mRNA expression in at least 2 cases.

Microarray analysis of *Ttc7* expression

We analyzed expression of *Ttc7*, the murine orthologue transcript, on hematopoietic and lymphoid tissues and on sorted T and B lymphoid cells with Mouse 430A 2.0 microarrays (Affymetrix, Santa Clara, Calif). As shown in Fig E5 in this article's Online Repository at www.jacionline.org, similar relative levels of *Ttc7* expression were identified in bone marrow, lymph nodes, and various T- and B-cell subpopulations; however, higher levels of expression were detected in total thymus.

Expression of TTC7A protein in normal thymus

Identification of high *Ttc7* expression in murine thymus and, to a lower extent, in lymphoid cells prompted us to extend this finding by analyzing TTC7A protein expression in human thymus. Immunostaining for TTC7A in normal human thymus demonstrated reactivity in a subset of cytokeratin-positive cortical and medullary thymic epithelial cells, with some signal present also in thymocytes (Fig 3). These results suggest that TTC7A might be involved in the normal biological function of these cells.

Severe lymphoid depletion in the thymus and peripheral lymphoid tissues of patients with CID-MIA

After confirming TTC7A expression in the thymus, we further examined the pathologic features of the thymus in patients with CID-MIA. Postmortem analysis of the thymus from patient F8-A revealed dysplastic changes, with vague corticomedullary demarcation and the presence of Hassall corpuscles, along with severe lymphoid depletion (see Fig E6, *A*, in this article's Online Repository at www.jacionline.org). Immunostaining for CD3 confirmed the marked reduction of thymocytes (see Fig E6, *B*).

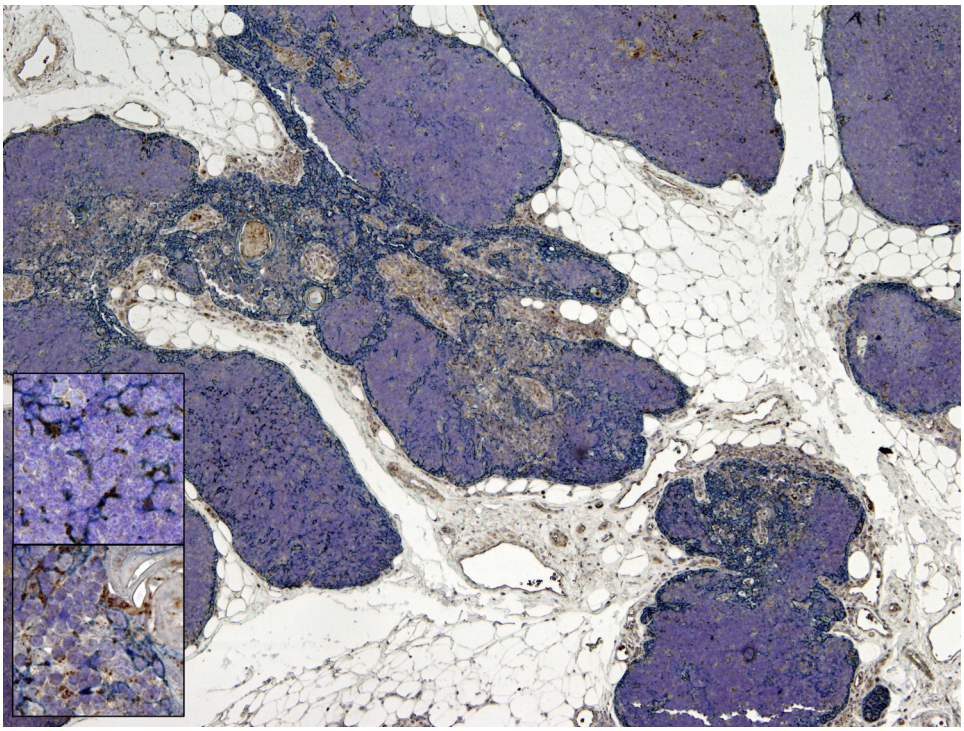

FIG 3. Immunostaining for TTC7A protein expression in normal thymus. Double immunostaining for cytokeratin *(blue)* and TTC7A *(brown)* shows scattered cytokeratin-positive epithelial cells in the cortex and in the medulla and a weaker but discernible signal in thymocytes (*upper inset*, detail of the cortex; *lower inset*, detail of the medulla). Magnification ×4 (inset ×20).

A mesenteric lymph node biopsy specimen from the same patient showed marked lymphoid depletion affecting both the cortex and the paracortex and a lack of follicles (see Fig E6, *C*), with a markedly reduced number of T and B lymphocytes (see Fig E7, *A* and *B*, in this article's Online Repository at www.jacionline.org). Similarly, marked lymphoid depletion was demonstrated in a mesenteric lymph node biopsy specimen from patient F7-A (see Fig E7, *C*).

DISCUSSION

In this study we identified deleterious mutations in the *TTC7A* gene in 8 patients with CID-MIA belonging to unrelated families of distinct ethnic origin, indicating a strong genetic link.

While we were preparing our manuscript, Samuels et al[27] reported on the occurrence of a homozygous 4-nt deletion (c.1000ΔAAGT) in 5 apparently unrelated French-Canadian patients with MIA and compound heterozygosity of exon 7 c.1000ΔAAGT + p.L823P (ie, exon 20 c.T2468C in our report) in 1 other affected patient. Their study cross-validated our findings that *TTC7A* might be the causal gene for SCID-MIA. The authors had postulated that the common occurrence of the exon 7 c.1000ΔAAGT mutation might reflect a founder effect in French-Canadian patients with MIA. Interestingly, the father of patient 5 (F5-A) was of French-Canadian origin, and the patient inherited this allele from him. Moreover, homozygosity for another mutation (exon 2 c.313ΔTATC) was identified in patients F2-A and F3-A, who are both of Slavian origin, possibly reflecting a founder effect among Slavians.

MIA can occur either isolated or in association with immunodeficiency. Among the patients reported by Samuels et al[27] with proved *TTC7A* mutations, only 1 was shown to have concurrent immunodeficiency with profound T-cell lymphopenia and hypogammaglobulinemia. By contrast, all patients included in this study presented with CID-MIA and carry *TTC7A* mutations, thus suggesting that biallelic mutations in this gene might account for both isolated multiple intestinal atresias and CID-MIA in affected subjects of different ethnic origin.

The exact incidence of severe immunodeficiency in patients with MIA is not known. The majority of the patients reported in the literature died early in life before accurate analysis of their immunologic status was performed. However, some of the data presented here might offer novel insights. In particular, patient F5-A from our series had extremely low TREC levels at birth. Retrospective analysis of TREC levels in dried blood spots collected at birth from other patients with MIA (with or without a confirmed diagnosis of associated immunodeficiency) might help to assess the actual incidence of severe T-cell immunodeficiency in this disease.

Immunologic studies in our patients have identified similarities but also some variability. In particular, 4 of our patients showed profound T-cell lymphopenia, which is consistent with a diagnosis of SCID. However, patient F1-A had only mild T-cell lymphopenia, and the majority of his circulating $CD4^+$ cells coexpressed CD45RA and CD31 markers,[28] suggesting partially preserved thymic function. On the other hand, profound $CD8^+$ T-cell lymphopenia was observed in all patients tested and might represent a more consistent phenotypic marker of impaired cell-mediated immunity and defective thymopoiesis.

Severe hypogammaglobulinemia was a common feature in our series and has been previously reported.[3-6,8,29] Interestingly, although all of the patients reported in this series had recurrent

and severe infections, the spectrum of infectious episodes differed from what is typically observed in patients with SCID, with fewer viral infections and a higher frequency of bloodstream infections caused by intestinal microbes. It is possible that this reflects abnormalities of the gut barrier in patients with CID-MIA.

Little is known about the expression and function of TTC7A, a member of a large family of proteins containing the tetratricopeptide repeat domain, which is defined by a degenerate consensus sequence of 34 amino acids.[30] Tetratricopeptide repeat domain–containing proteins, such as TTC7A, have diverse functions in cell-cycle control, protein transport, phosphate turnover, and protein trafficking or secretion, and they can act as chaperones or scaffolding proteins.[31] *TTC7A* has been shown to be expressed more abundantly in the thymus and colon and in colorectal adenocarcinoma cells.[32] Spontaneous mutations in the murine *TTC7A* orthologue *Ttc7* have been identified in the *flaky skin (fsn)* mouse,[33-38] the hereditary erythroblastic anemia *(hea)* mouse,[31,39] and the *Ttc7*$^{fsn\text{-}Jic}$ mouse.[40,41] These mouse models show anemia, skin abnormalities, and immune dysregulation but not intestinal atresias, although forestomach epithelial hyperplasia is present in *fsn* mice. It is plausible that the actual function of the human TTC7A protein and its murine orthologue, Ttc7, might have diversified during evolution, although they share 88% amino acid sequence homology (see Fig E8 in this article's Online Repository at www.jacionline.org).

We have demonstrated abundant expression of TTC7A in a subset of cortical and medullary thymic epithelial cells and in Hassall corpuscles and lower but clearly discernible expression in thymocytes. Microarray analysis of expression of the murine orthologue *Ttc7* confirmed higher relative levels of expression in the thymus. Postmortem analysis of the thymus from patient F8-A showed severe lymphoid depletion and vague corticomedullary demarcation, with preserved presence of Hassall corpuscles. Moreover, severe lymphoid depletion, affecting both T and B cells, was demonstrated in peripheral lymph nodes from patients F7-A and F8-A. Overall, these findings are consistent with the notion that mutations of the *TTC7A* gene affect immune system development and function and hence cause the combined immunodeficiency associated with MIA. Defining whether the severe immunodeficiency seen in patients with CID-MIA is intrinsic to lymphoid cells or whether it is mainly due to extrahematopoietic defects would have important therapeutic implications. Most patients with CID-MIA die early in life, and there is very limited experience with attempts to achieve immune reconstitution in this disease. Samuels et al[27] have reported on an infant with CID-MIA who received an HLA-matched cord blood transplantation at 6.5 months of age but died at 1 year of age. Patient F6-A in our series received HCT from a matched unrelated donor on conditioning with cyclophosphamide and thiotepa but also died early after transplantation. By contrast, patient F5-A in this study received a well-matched HCT without preparative chemotherapy and has achieved donor T-cell engraftment. Although the presence of T cells with a naive phenotype suggests effective *de novo* thymopoiesis, longer follow-up studies will be needed to confirm the efficacy of HCT. Finally, donor-derived, partial immune reconstitution has been observed after combined liver and small bowel transplantation in another infant with CID-MIA.[29] Interestingly, in this case, almost all T cells were of donor origin, and were either $CD4^{-}CD8^{-}TCR\gamma\delta^{+}$ or $CD3^{-}CD4^{-}CD8\alpha\alpha^{+}$, which is indicative of a possible intestinal intraepithelial origin. Although the function of TTC7A has yet to be defined, it might be a key factor to bridge the 2 processes of both immune system and digestive tract development.

We thank the patients and the families for their collaboration. Raw sequencing reads can be accessed at the National Center for Biotechnology Information database of Genotypes and Phenotypes (dbGaP). Accession numbers will be available before publication of the article.

Clinical implications: Damaging mutations in the gene *TTC7A* should be scrutinized in patients with CID-MIA. Characterization of the role of this protein in the immune system and intestinal development, as well as in thymic epithelial cells, might have important therapeutic implications.

REFERENCES

1. Guttman FM, Braun P, Garance PH, Blanchard H, Collin PP, Dallaire L, et al. Multiple atresias and a new syndrome of hereditary multiple atresias involving the gastrointestinal tract from stomach to rectum. J Pediatr Surg 1973;8:633-40.
2. Mishalany HG, Der Kaloustian VM. Familial multiple-level intestinal atresias: report of two siblings. J Pediatr 1971;79:124-5.
3. Moreno LA, Gottrand F, Turck D, Manouvrier-Hanu S, Mazingue F, Morisot C, et al. Severe combined immunodeficiency syndrome associated with autosomal recessive familial multiple gastrointestinal atresias: study of a family. Am J Med Genet 1990;37:143-6.
4. Rothenberg ME, White FV, Chilmonczyk B, Chatila T. A syndrome involving immunodeficiency and multiple intestinal atresias. Immunodeficiency 1995;5:171-8.
5. Ali YA, Rahman S, Bhat V, Al Thani S, Ismail A, Bassiouny I. Hereditary multiple intestinal atresia (HMIA) with severe combined immunodeficiency (SCID): a case report of two siblings and review of the literature on MIA, HMIA and HMIA with immunodeficiency over the last 50 years. BMJ Case Rep 2011;2011.
6. Moore SW, de Jongh G, Bouic P, Brown RA, Kirsten G. Immune deficiency in familial duodenal atresia. J Pediatr Surg 1996;31:1733-5.
7. Cole C, Freitas A, Clifton MS, Durham MM. Hereditary multiple intestinal atresias: 2 new cases and review of the literature. J Pediatr Surg 2010;45:E21-4.
8. Walker MW, Lovell MA, Kelly TE, Golden W, Saulsbury FT. Multiple areas of intestinal atresia associated with immunodeficiency and posttransfusion graft-versus-host disease. J Pediatr 1993;123:93-5.
9. Reyes J, Todo S, Green M, Yunis E, Schoner D, Kocoshis S, et al. Graft-versus-host disease after liver and small bowel transplantation in a child. Clin Transpl 1997;11:345-8.
10. Dallaire L, Perreault G. Hereditary multiple intestinal atresia. Birth Defects Orig Artic Ser 1974;10:259-64.
11. Bilodeau A, Prasil P, Cloutier R, Laframboise R, Meguerditchian AN, Roy G, et al. Hereditary multiple intestinal atresia: thirty years later. J Pediatr Surg 2004;39:726-30.
12. Arnal-Monreal F, Pombo F, Capdevila-Puerta A. Multiple hereditary gastrointestinal atresias: study of a family. Acta Paediatr Scand 1983;72:773-7.
13. Gungor N, Balci S, Tanyel FC, Gogus S. Familial intestinal polyatresia syndrome. Clin Genet 1995;47:245-7.
14. Gahukamble DB, Adnan AR, Al-Gadi M. Atresias of the gastrointestinal tract in an inbred, previously unstudied population. Pediatr Surg Int 2002;18:40-2.
15. Gahukamble DB, Gahukamble LD. Multiple gastrointestinal atresias in two consecutive siblings. Pediatr Surg Int 2002;18:175-7.
16. Chen R, Snyder M. Systems biology: personalized medicine for the future? Curr Opin Pharmacol 2012;12:623-8.
17. Clark MJ, Chen R, Lam HY, Karczewski KJ, Chen R, Euskirchen G, et al. Performance comparison of exome DNA sequencing technologies. Nat Biotechnol 2011;29:908-14.
18. Mias G, Snyder M. Personal genomes, quantitative dynamic omics and personalized medicine. Quant Biol 2013;1:71-90.
19. Li H, Durbin R. Fast and accurate short read alignment with Burrows-Wheeler transform. Bioinformatics 2009;25:1754-60.
20. McKenna A, Hanna M, Banks E, Sivachenko A, Cibulskis K, Kernytsky A, et al. The Genome Analysis Toolkit: a MapReduce framework for analyzing next-generation DNA sequencing data. Genome Res 2010;20:1297-303.
21. DePristo MA, Banks E, Poplin R, Garimella KV, Maguire JR, Hartl C, et al. A framework for variation discovery and genotyping using next-generation DNA sequencing data. Nat Genet 2011;43:491-8.
22. Green MR, Monti S, Dalla-Favera R, Pasqualucci L, Walsh NC, Schmidt-Supprian M, et al. Signatures of murine B-cell development implicate Yy1 as a

regulator of the germinal center-specific program. Proc Natl Acad Sci U S A 2011;108:2873-8.
23. Hale JE, Bonilla FA, Pai SY, Gerstel-Thompson JL, Notarangelo LD, Eaton RB, et al. Identification of an infant with severe combined immunodeficiency by newborn screening. J Allergy Clin Immunol 2010;126:1073-4.
24. Krzywinski M, Schein J, Birol I, Connors J, Gascoyne R, Horsman D, et al. Circos: an information aesthetic for comparative genomics. Genome Res 2009;19:1639-45.
25. 1000 Genomes Project Consortium, Abecasis GR, Auton A, Brooks LD, DePristo MA, Durbin RM, et al. An integrated map of genetic variation from 1,092 human genomes. Nature 2012;491:56-65.
26. Exome Variant Server, NHLBI GO Exome Sequencing Project (ESP). Available at: http://evs.gs.washington.edu/EVS/. Accessed May 21, 2013.
27. Samuels ME, Majewski J, Alirezaie N, Fernandez I, Casals F, Patey N, et al. Exome sequencing identifies mutations in the gene TTC7A in French-Canadian cases with hereditary multiple intestinal atresia. J Med Genet 2013;50:324-9.
28. Kimmig S, Przybylski GK, Schmidt CA, Laurisch K, Mowes B, Radbruch A, et al. Two subsets of naive T helper cells with distinct T cell receptor excision circle content in human adult peripheral blood. J Exp Med 2002;195:789-94.
29. Gilroy RK, Coccia PF, Talmadge JE, Hatcher LI, Pirruccello SJ, Shaw BW Jr, et al. Donor immune reconstitution after liver-small bowel transplantation for multiple intestinal atresia with immunodeficiency. Blood 2004;103:1171-4.
30. Blatch GL, Lassle M. The tetratricopeptide repeat: a structural motif mediating protein-protein interactions. Bioessays 1999;21:932-9.
31. White RA, McNulty SG, Nsumu NN, Boydston LA, Brewer BP, Shimizu K. Positional cloning of the Ttc7 gene required for normal iron homeostasis and mutated in hea and fsn anemia mice. Genomics 2005;85:330-7.
32. Wu C, Orozco C, Boyer J, Leglise M, Goodale J, Batalov S, et al. BioGPS: an extensible and customizable portal for querying and organizing gene annotation resources. Genome Biol 2009;10:R130.
33. Helms C, Pelsue S, Cao L, Lamb E, Loffredo B, Taillon-Miller P, et al. The tetratricopeptide repeat domain 7 gene is mutated in flaky skin mice: a model for psoriasis, autoimmunity, and anemia. Exp Biol Med 2005;230:659-67.
34. Abernethy NJ, Hagan C, Tan PL, Birchall NM, Watson JD. The peripheral lymphoid compartment is disrupted in flaky skin mice. Immunol Cell Biol 2000;78:5-12.
35. Pelsue SC, Schweitzer PA, Schweitzer IB, Christianson SW, Gott B, Sundberg JP, et al. Lymphadenopathy, elevated serum IgE levels, autoimmunity, and mast cell accumulation in flaky skin mutant mice. Eur J Immunol 1998;28:1379-88.
36. Mattsson N, Duzevik EG, Pelsue SC. Expansion of CD22lo B cells in the spleen of autoimmune-prone flaky skin mice. Cell Immunol 2005;234:124-32.
37. Welner R, Swett DJ, Pelsue SC. Age-related loss of bone marrow pre-B- and immature B-lymphocytes in the autoimmune-prone flaky skin mutant mice. Autoimmunity 2005;38:399-408.
38. Welner R, Hastings W, Hill BL, Pelsue SC. Hyperactivation and proliferation of lymphocytes from the spleens of flaky skin (fsn) mutant mice. Autoimmunity 2004;37:227-35.
39. Shimizu K, Keino H, Ogasawara N, Esaki K. Hereditary erythroblastic anaemia in the laboratory mouse. Lab Anim 1983;17:198-202.
40. Takabayashi S, Katoh H. A mutant mouse with severe anemia and skin abnormalities controlled by a new allele of the flaky skin (fsn) locus. Exp Anim 2005;54:339-47.
41. Takabayashi S, Iwashita S, Hirashima T, Katoh H. The novel tetratricopeptide repeat domain 7 mutation, Ttc7fsn-Jic, with deletion of the TPR-2B repeat causes severe flaky skin phenotype. Exp Biol Med 2007;232:695-9.

METHODS

WES

The SureSelect Human All Exon Kit 50M (Agilent Technologies) was used to prepare Illumina sequencing libraries, as reported previously,[E1] according to the manufacturer's instructions. Briefly, 3 μg of high-quality (average size, >40 kb; A260/A280, >1.8) genomic DNA was fragmented with the Covaris S2 system (Invitrogen, Carlsbad, Calif); DNA fragments were end-repaired, and a deoxyadenosine base was added to the 3′ ends of the fragments, ligated with paired-end adaptors, and amplified by PCR (4 cycles). Amplified, adaptor-ligated libraries were then hybridized for 24 hours with biotinylated oligo RNA baits for targeted exomic regions and enriched with streptavidin-conjugated magnetic beads. The enriched libraries were further amplified for 11 cycles with indexed primers and subjected to Illumina sequencing by multiplexing 2 libraries per lane of the HiSeq 2000 sequencer. The final libraries were denatured with sodium hydroxide and loaded onto an Illumina cBot for cluster generation, and the primer-hybridized flow cells were then transferred to HiSeq 2000 sequencers for paired-end 101 b sequencing.

WES data analysis

Paired-end, 101 b short reads generated from each library were aligned to the reference genome GRCh37 with the Burrows-Wheeler Aligner (version 0.6.0).[E2] The parameter −q 30 was used to allow soft clipping. The aligned reads were converted to the BAM format with SAMtools (version 0.1.12a)[E3] and sorted, and duplicate reads were removed by using Picard (http://picard.sourceforge.net, version 1.46, MarkDuplicates). Read group information was subsequently added to a BAM header by Picard (AddOrReplaceReadGroups), which was required for downstream processing with the GATK. Insertions and/or deletions (Indels) were locally realigned with GATK (version 1.3-17-gc62082b),[E4,E5] followed by FixMateInformation with Picard, and variants were called by using the GATK UnifiedGenotyper. Called SNV and Indel variants were further annotated with ANNOVAR (version 2013Feb21),[E6] and potentially damaging Indels were predicted with the SIFT online tool (http://sift.jcvi.org/www/SIFT_chr_coords_indels_submit.html).[E7]

RNA analysis of human samples

RT-PCR was performed to amplify exons 4 to 12 on cDNA prepared from induced pluripotent stem cells from a control subject and patient F5-A by using primers spanning the exon 4-5 junction (5′-CTGCAGGAATTGGA GAAGACC-3′) and the exon 11-12 junction (5′-GTGCTCTGCTTCCT CTAGCC-3′).

RT-PCR analysis in patient F8-A was performed by amplifying the whole *TTC7A* open reading frame on cDNA prepared from PBMCs using primers spanning exons 1 to 4 (1F-5′-TCTTGGCCGCACCTTCCAT-3′; 4R-5′-TCC TCCCTCTCTGTCAGG-3′), exons 4 to 12 (4F-5′-CTCTCTCTGGAAC GCCTAC-3′; 12R-5′-AGGTAGCCCTTGGGGAGG-3′), and exons 12 to 20 (12F-5′-GGAAGCAGAGCACTTTGCC-3′; 20R-5′-CTCCCTGCGGCTGC AGC-3′).

Immunohistochemistry analysis of TTC7A expression in human tissues

Four-micrometer sections of tissues of paraffin-embedded normal thymus were stained with hematoxylin and eosin and immunostained with anti-TTC7A (rabbit polyclonal, dilution 1:25, overnight incubation; Sigma, St Louis, Mo) on heat-based antigen retrieval in citrate buffer, pH 6.0, by using a microwave oven. Reactivity was revealed with the horseradish peroxidase–linked NovoLink Polymer (Leica Microsystems, Buffalo Grove, Ill), followed by diaminobenzidine. Slides were counterstained with Mayer hematoxylin. Sections from postmortem paraffin-embedded thymus, inguinal lymph node, and spleen tissue from patient F8-A and a mesenteric lymph node biopsy specimen from patient F7-A were stained with hematoxylin and eosin and immunostained for CD3 (rabbit monoclonal anti-CD3, clone SP7, dilution 1:100; Thermo Scientific, West Palm Beach, Fla) and CD20 (mouse monoclonal anti-CD20, clone L26, dilution 1:250, Leica Microsystems). Reactivity was revealed as described above. For double immunostaining, after completing the first immune reaction for TTC7A, anti-cytokeratin (mouse monoclonal, clone MNF116, dilution 1:100; Dako, Glostrup, Denmark) was applied, and the immune reaction was visualized with alkaline phosphatase–linked Mach4 (Biocare Medical, Concord, Calif), followed by Ferangi Blue (Biocare Medical) as the chromogen.

Microarray analysis of murine *Ttc7* mRNA expression

Whole bone marrow was obtained as the cellular portion derived from mortar and pestle–ground femurs of mice. Whole mouse thymus was disrupted to single cells, and total RNA was extracted. Murine bone marrow and peripheral lymphoid cells were sorted, as previously described.[E8] Total RNA was amplified to cRNA by using the Ovation RNA Amplification system V2 (NuGen Technologies, San Carlos, Calif), according to the manufacturer's protocol. Total cRNA was labeled with the Affymetrix Gene Chip Labeling Kit (Affymetrix), hybridized overnight on Mouse 430A 2.0 microarrays (Affymetrix), washed, and imaged, as per the manufacturer's protocol. For each cell population, at least 3 separate purifications were performed.

RESULTS

WES statistics

A summary of sequencing statistics is listed in Table E3. In brief, an average of 18 Gb of sequence was generated per library from approximately 91M paired-end reads (Table E3), which covered an average of 87 million bases of the human genome. Of the called bases, 50.6 to 51.6 Mb are on-capture-target base calls, of which a range of 38.3 to 47.3 Mb had at least 30X depth of coverage. The median depth of coverage for each library ranges from 57X to 178X. A more detailed summary of numbers of bases called at different depths of coverage is listed in Table E4.

We next identified SNVs and Indels by using the GATK.[E4,E5] A total of 109,877 variants were called in the exomes of all subjects, including 100,587 SNVs and 9,290 Indels (Fig 1, *B*, and Table E5). Each sequenced exome contains an average of 44,468 (42,982-45,296) SNVs and 4,717 (4,645-4,850) Indels. The average transition/transversion ratio is 2.54 (2.50-2.57), which is similar to that observed previously in unrelated human exomes.[E1] The length of the called Indels ranges from −52 bp to +35 bp, with 83.6% and 93.4% of Indels (with quality score higher than the lower quartile) falling in length ranges of approximately −3 bp to +3 bp and −6 bp to +6 bp, respectively (Fig E9).

We further screened for variants that followed various potential modes of inheritance for this disease in each of the 5 core families. A total of 5 modes of inheritance were considered: autosomal recessive, X-linked recessive, pseudoautosomal, germline *de novo*, and compound heterozygous (Table E6). Potentially damaging variants were subsequently identified based on several criteria (not-in-segment duplication regions, nonsynonymous/stop-gain/stop-loss, and 1000 Genome Projects minor allele frequency ≤0.05; Table E5) and further examined by using SIFT (<0.05),[E7] PolyPhen-2 (>0.85),[E9] and SIFT Indel prediction (Cause NMD = "yes") scores.

REFERENCES

E1. Clark MJ, Chen R, Lam HY, Karczewski KJ, Chen R, Euskirchen G, et al. Performance comparison of exome DNA sequencing technologies. Nat Biotechnol 2011;29:908-14.

E2. Li H, Durbin R. Fast and accurate short read alignment with Burrows-Wheeler transform. Bioinformatics 2009;25:1754-60.

E3. Li H, Handsaker B, Wysoker A, Fennell T, Ruan J, Homer N, et al. The sequence alignment/map format and SAMtools. Bioinformatics 2009;25:2078-9.

E4. McKenna A, Hanna M, Banks E, Sivachenko A, Cibulskis K, Kernytsky A, et al. The Genome Analysis Toolkit: a MapReduce framework for analyzing next-generation DNA sequencing data. Genome Res 2010;20:1297-303.

E5. DePristo MA, Banks E, Poplin R, Garimella KV, Maguire JR, Hartl C, et al. A framework for variation discovery and genotyping using next-generation DNA sequencing data. Nat Genet 2011;43:491-8.

E6. Wang K, Li M, Hakonarson H. ANNOVAR: functional annotation of genetic variants from high-throughput sequencing data. Nucleic Acids Res 2010;38:e164.

E7. Kumar P, Henikoff S, Ng PC. Predicting the effects of coding non-synonymous variants on protein function using the SIFT algorithm. Nat Protoc 2009;4:1073-81.

E8. Green MR, Monti S, Dalla-Favera R, Pasqualucci L, Walsh NC, Schmidt-Supprian M, et al. Signatures of murine B-cell development implicate Yy1 as a regulator of the germinal center-specific program. Proc Natl Acad Sci U S A 2011; 108:2873-8.

E9. Adzhubei IA, Schmidt S, Peshkin L, Ramensky VE, Gerasimova A, Bork P, et al. A method and server for predicting damaging missense mutations. Nat Methods 2010;7:248-9.

E10. White RA, McNulty SG, Nsumu NN, Boydston LA, Brewer BP, Shimizu K. Positional cloning of the Ttc7 gene required for normal iron homeostasis and mutated in hea and fsn anemia mice. Genomics 2005;85:330-7.

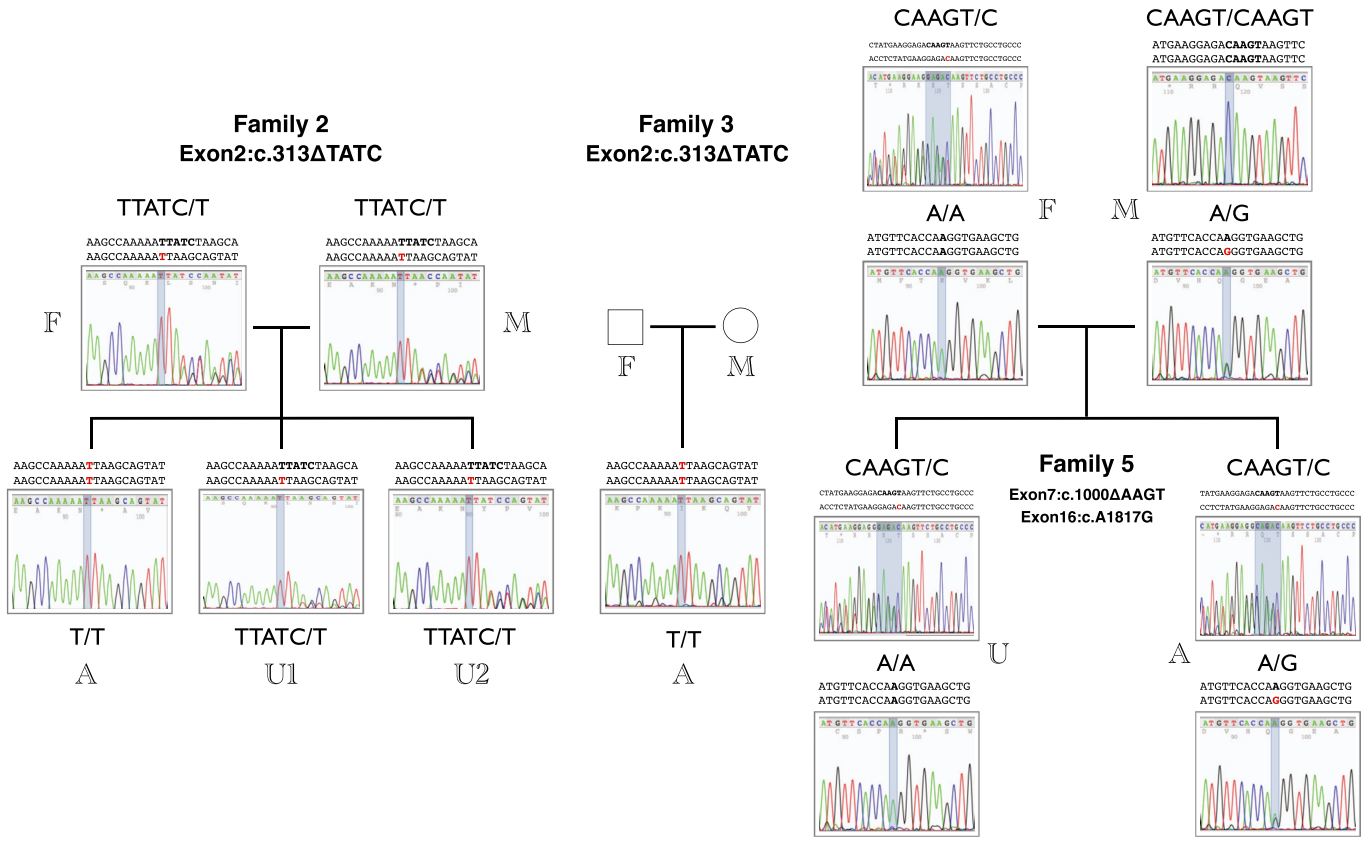

FIG E1. Sanger sequencing validation of *TTC7A* mutations in families 2, 3, and 5.

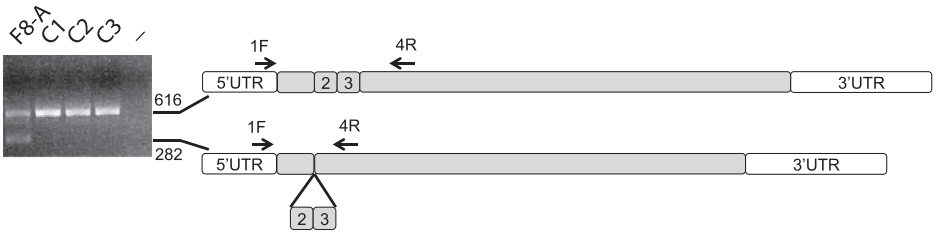

FIG E2. *TTC7A* mRNA aberrant splicing in patient F8-A. cDNA of the *TTC7A* gene was amplified and sequenced. Using a forward primer in exon 1 and a reverse primer in exon 4, we detected a normal-sized cDNA and an in-frame cDNA product lacking exons 2 and 3. *UTR*, Untranslated region.

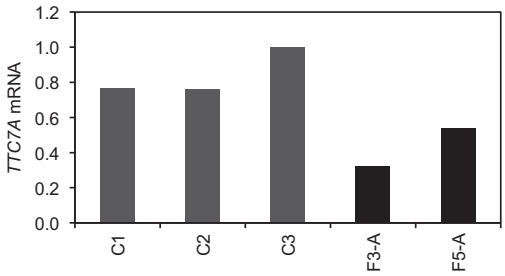

FIG E3. *TTC7A* gene expression in fibroblasts of patients F3-A and F5-A. Expression levels were normalized to expression of the housekeeping gene glyceraldehyde-3-phosphate dehydrogenase *(GAPDH)* and compared to levels of expression in fibroblasts from 3 unrelated healthy control subjects (*C1*, *C2*, and *C3*).

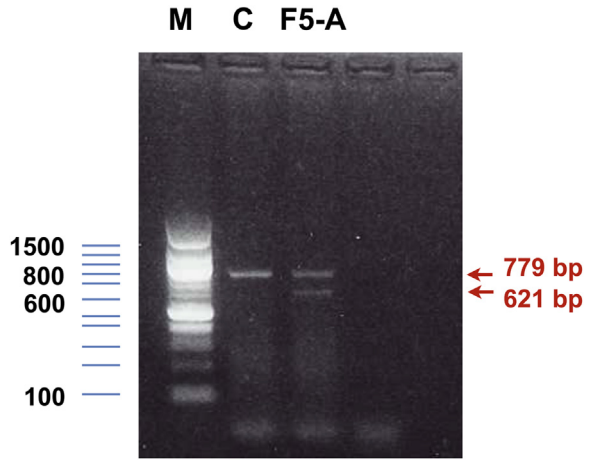

FIG E4. RT-PCR amplification for exons 4 to 12 of the *TTC7A* gene in patient 5 (F5-A). cDNA prepared from induced pluripotent stem cells from a healthy control subject *(C)* who does not harbor the exon 7 c.1000ΔAAGT mutation and patient 5 (F5-A) were amplified by using primers spanning the exon 4-5 junction (5′CTGCAGGAATTGGAGAAGACC3′) and the exon 11-12 junction (5′GTGCTCTGCTTCCTCTAGCC3′). The expected wild-type band is 779 bp, with the band skipping exon 7 expected to be 621 bp. Note that the control sample has only the wild-type band, whereas patient F5-A has both bands, indicating the skipping of exon 7. *M*, DNA ladder.

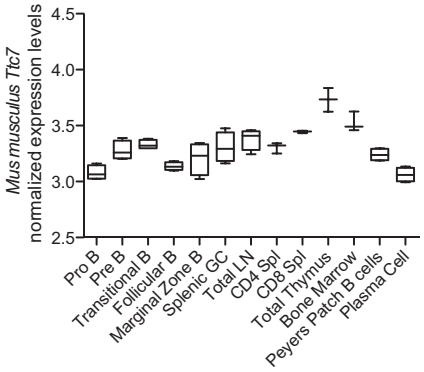

FIG E5. Relative probe intensity with standard deviation for *Ttc7* transcripts in sorted lymphocyte populations, as well as in total thymus, bone marrow, and lymph node *(LN)* tissue. *GC*, Germinal center.

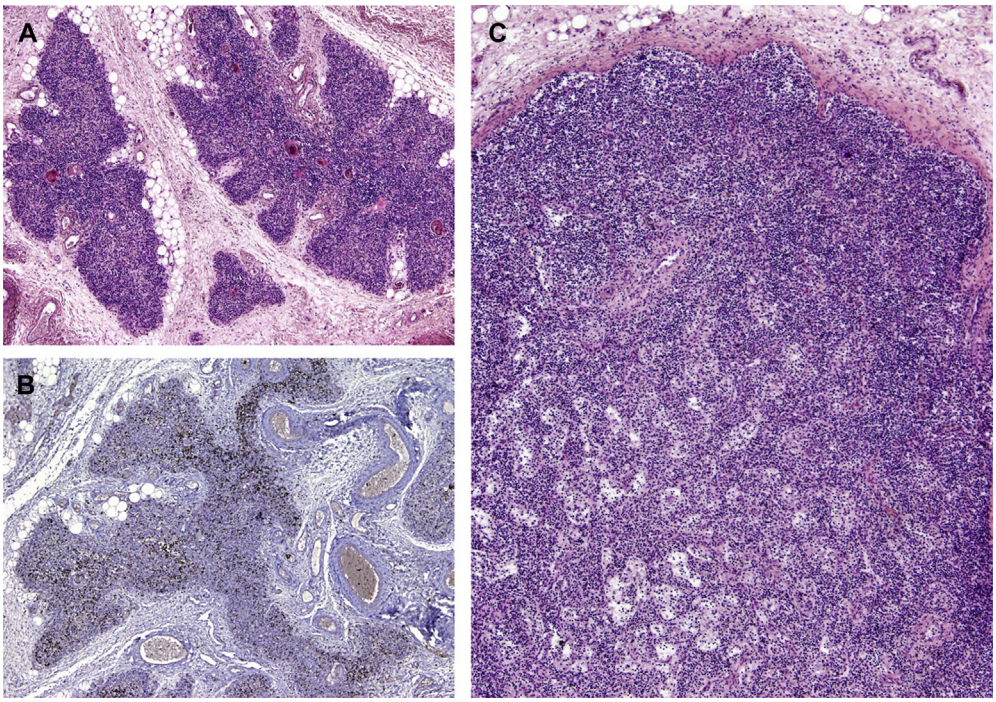

FIG E6. Thymic and lymph node abnormalities in patient F8-A. **A,** Postmortem analysis of the thymus shows severe lymphoid depletion, with a vague corticomedullary demarcation but preserved presence of Hassall corpuscles. **B,** Staining for CD3 in the thymus of patient F8-A showed marked depletion of thymocytes. **C,** Marked lymphoid depletion affecting both the cortex and the paracortex and lack of follicles in mesenteric lymph nodes. Fig E6, *A* and *B*, Magnification ×4; Fig E6, *C*, magnification ×10.

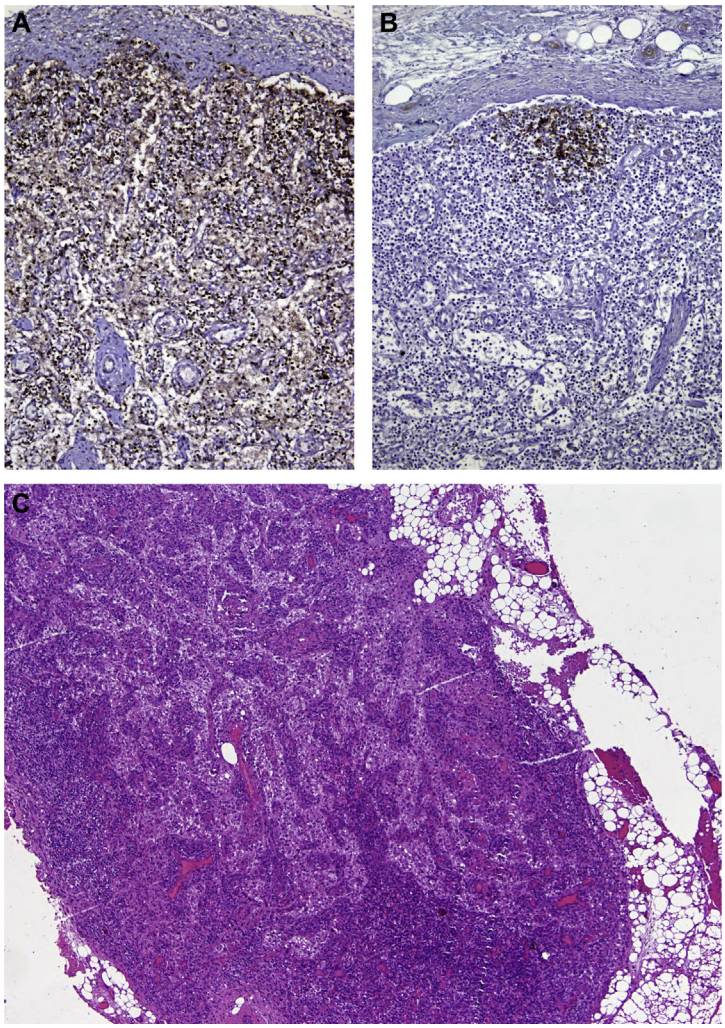

FIG E7. Staining of a mesenteric lymph node from patient F8-A shows marked depletion of $CD3^+$ cells **(A)** and $CD20^+$ B lymphocytes (**B**; magnification ×10). **C,** Hematoxylin and eosin staining of a mesenteric lymph node from patient F7-A shows marked lymphoid depletion (magnification ×4).

IDENTITIES : 88% (758 / 859)
POSITIVES : 94% (811 / 859)

```
TTC7A (Home sapiens)  1    MAAKGAHGSYLKVESELERCRAEGHWDRMPELVRQLQTLSMPGGGG-NRRGSPSAAFTFP  59
                           MAAKGAHG++LKVESE+ERCRAEG WDRM EL R LQ L + GGG  NRR SPS  FT
Ttc7  (Mus musculus)  1    MAAKGAHGTHLKVESEVERCRAEGQWDRMFELARHLQMLGISGGGSSNRRNSPSGRFTTL  60

TTC7A (Home sapiens)  60   DTDDFGKLLLAEALLEQCLKENHAKIKDSMPLLEKNEPKMSEAKNYLSSILNHGRLSPQY  119
                           DTDDF KLLLAEALLEQCLK+NH KIK+S+PLLEK + +++EAK++LSS+LN+G+L PQY
Ttc7  (Mus musculus)  61   DTDDFVKLLLAEALLEQCLKDNHDKIKNSIPLLEKTDHRLNEAKDHLSSLLNNGKLPPQY  120

TTC7A (Home sapiens)  120  MCEAMLILGKLHYVEGSYRDAISMYARAGIDDMSMENKPLYQMRLLSEAFVIKGLSLERL  179
                           MCEAMLILGKLHYVEGSYRDA+SMYARAGIDD+S+ENKPLYQMRLLSEAFVIKGLSLERL
Ttc7  (Mus musculus)  121  MCEAMLILGKLHYVEGSYRDAVSMYARAGIDDISVENKPLYQMRLLSEAFVIKGLSLERL  180

TTC7A (Home sapiens)  180  PNSIASRFRLTEREEEVITCFERASWIAQVFLQELEKTTNNSTSRHLKGCHPLDYELTYF  239
                           PNS+AS  RLTEREEEV+ CFERASW+AQVFLQELEKT+NNSTSRHLKG    DYEL+YF
Ttc7  (Mus musculus)  181  PNSVASHIRLTEREEEVVACFERASWVAQVFLQELEKTSNNSTSRHLKGSLSPDYELSYF  240

TTC7A (Home sapiens)  240  LEAALQSAYVKNLKKGNIVKGMRELREVLRTVETKATQNFKVMAAKHLAGVLLHSLSEEC  299
                           LEAALQSAYVKNLKKGNIVKGMRELRE+LRTVETKATQNFKV+AAKHLAGVLLHSLSE+C
Ttc7  (Mus musculus)  241  LEAALQSAYVKNLKKGNIVKGMRELREILRTVETKATQNFKVVAAKHLAGVLLHSLSEDC  300

TTC7A (Home sapiens)  300  YWSPLSHPLPEFMGKEESSFATQALRKPHLYEGDNLYCPKDNIEEALLLLLISESMATRD  359
                           YWSPLSHPLPEFM KEE+SF TQ LRKPHLYEGDNLYCPKDNIEEALLLLLISESMATRD
Ttc7  (Mus musculus)  301  YWSPLSHPLPEFMNKEENSFVTQTLRKPHLYEGDNLYCPKDNIEEALLLLLISESMATRD  360

TTC7A (Home sapiens)  360  VVLSRVPEQEEDRTVSLQNAAAIYDLLSITLGRRGQYVMLSECLERAMKFAFGEFHLWYQ  419
                           VVLSR PEQ EDR VSLQNA+AIYDLLSITLGRRGQYVMLSECLERAMK AFGEFHLWYQ
Ttc7  (Mus musculus)  361  VVLSRAPEQAEDRKVSLQNASAIYDLLSITLGRRGQYVMLSECLERAMKCAFGEFHLWYQ  420

TTC7A (Home sapiens)  420  VALSMVACGKSAYAVSLLRECVKLRPSDPTVPLMAAKVCIGSLRWLEEAEHFAMMVISLG  479
                           VALSMVACGKSAYAVSLLREC+KL+PSDPTVPLMAAKVCIGSL WLEEAEHFA +VI LG
Ttc7  (Mus musculus)  421  VALSMVACGKSAYAVSLLRECMKLQPSDPTVPLMAAKVCIGSLHWLEEAEHFATVVIGLG  480

TTC7A (Home sapiens)  480  EEAGEFLPKGYLALGLTYSLQATDATLKSKQDELHRKALQTLERAQQLAPSDPQVILYVS  539
                           EEAGE LPKGYLALGLTYSLQATDATLKSKQDELHRKALQTLERA++LAP DPQ+I YV+
Ttc7  (Mus musculus)  481  EEAGESLPKGYLALGLTYSLQATDATLKSKQDELHRKALQTLERARELAPDDPQIIFYVA  540

TTC7A (Home sapiens)  540  LQLALVRQISSAMEQLQEALKVRKDDAHALHLLALLFSAQKHHQHALDVVNMAITEHPEN  599
                           LQLALVRQISSAME+LQEAL + +DDA+ALHLLALLFSAQK++QHALDV+NMAITEHPEN
Ttc7  (Mus musculus)  541  LQLALVRQISSAMERLQEALTMCRDDANALHLLALLFSAQKYYQHALDVINMAITEHPEN  600

TTC7A (Home sapiens)  600  FNLMFTKVKLEQVLKGPEEALVTCRQVLRLWQTLYSFSQLGGLEKDGSFGEGLTMKKQSG  659
                           FNLMFTKVKLEQVLKGPEEALVTCRQ+LRLWQTLY+FSQLGGLEKDGSF EGLT+KKQ+G
Ttc7  (Mus musculus)  601  FNLMFTKVKLEQVLKGPEEALVTCRQMLRLWQTLYNFSQLGGLEKDGSF-EGLTVKKQNG  659

TTC7A (Home sapiens)  660  MHLTLPDAHDADSGSRRASSIAASRLEEAMSELTMPSSVLKQGPMQLWTTLEQIWLQAAE  719
                           +HLTLPDAHDADSGSRRASSIAASRLEEAMSELT+ +SVLKQGPMQLWTTLEQIWLQAAE
Ttc7  (Mus musculus)  660  IHLTLPDAHDADSGSRRASSIAASRLEEAMSELTLTTSVLKQGPMQLWTTLEQIWLQAAE  719

TTC7A (Home sapiens)  720  LFMEQQHLKEAGFCIQEAAGLFPTSHSVLYMRGRLAEVKGNLEEAKQLYKEALTVNPDGV  779
                           LFMEQ+ LKEAGFCIQEAAGLFPTSHSVLYMRGRLAEVKG+ EEAKQLYKEALTVNPDGV
Ttc7  (Mus musculus)  720  LFMEQRQLKEAGFCIQEAAGLFPTSHSVLYMRGRLAEVKGSFEEAKQLYKEALTVNPDGV  779

TTC7A (Home sapiens)  780  RIMHSLGLMLSRLGHKSLAQKVLRDAVERQSTCHEAWQGLGEVLQAQGQNEAAVDCFLTA  839
                           RIMHSLGLMLS+LGHKSLAQKVLRDAVERQST HEAWQGLGEVLQ QGQNEAAVDCFLTA
Ttc7  (Mus musculus)  780  RIMHSLGLMLSQLGHKSLAQKVLRDAVERQSTFHEAWQGLGEVLQDQGQNEAAVDCFLTA  839

TTC7A (Home sapiens)  840  LELEASSPVLPFSIIPREL  858
                           LELEASSPVLPFSII REL
Ttc7  (Mus musculus)  840  LELEASSPVLPFSIIAREL  858
```

FIG E8. Comparison of the protein sequences of human and mouse TTC7A orthologues using Basic Local Alignment Search Tool[E10] from the National Center for Biotechnology Information.

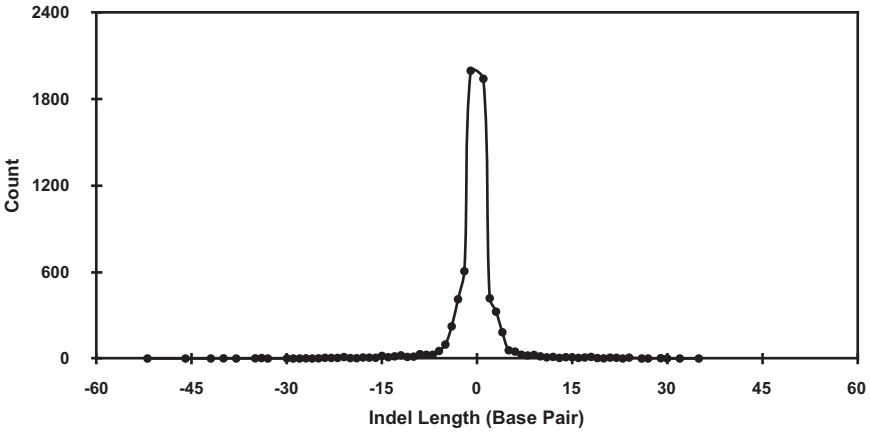

FIG E9. Distribution of the length of Indels identified by using WES.

TABLE E1. Sanger sequencing validation PCR primer information

Family no.	No. of chromosomes	POS	REF	ALT	Primer-F	Tm-F (C)	Primer-R	Tm-R (C)	Product length (bp)	Single band product?
1	2	47273571	G	A	CCTCATGGCACTCTGCTTTCT	61.9	CTCTATGTACTTCATAGAGGACTGTCA	57.4	444	No
2	2	47177629	TTATC	T	GGGAAATTGCTGCTGGCTGA	65.8	GTAAGAGAGACTTGTTGCTCAGGTGA	62.4	266	Yes
3	2	47177629	TTATC	T	GGGAAATTGCTGCTGGCTGA	65.8	GTAAGAGAGACTTGTTGCTCAGGTGA	62.4	266	Yes
4	2	47206043	AG	A	CACCTCCTCTTGCTGAGTGACC	63.6	CACCAATCCTCTTGGAAGAGCAC	64.4	316	No
4	2	47300953	T	C	GTCTGATGCTGAGTCGGCTG	62.2	CACGTTCCCTGCTGCCTCT	63.9	280	No
5	2	47221651	CAAGT	C	CTGAGTGAGGAGTGCTACTGGAG	60.6	CCTGCTGAGACTGAGGAGGCT	63.5	263	Yes
5	2	47273468	A	G	GCGAGTTAGGGAGGTGAGCA	62.8	GAGACAATGACGGCCACTCA	62.3	244	Yes
5	2	47277182	T	C	CCTCTACCTTACCGGACCCTG	62.1	CCTACCCAGAGCCAAGATCAG	61.1	307	Yes

ALT, Alternative sequence; *POS*, position; *REF*, reference sequence.

TABLE E2. Immune reconstitution after HCT in patient 5

Days after HCT	CD3 (cells/μL)	CD4 (cells/μL)	CD8 (cells/μL)	$CD19^+$ (cells/μL)	$CD16^+CD56^+$ (cells/μL)	$CD4^+CD45RA^+$ $CCR7^+$ (cells/μL)	$CD4^+CD45RA^-$ (cells/μL)	Donor T-cell chimerism (%)	PHA (cpm)	IgG (mg/dL)	IgA (mg/dL)	IgM (mg/dL)
Pre-HCT	74	49	14	458	118	12	37	–	2,487	<75	<6	5
19	442	361	69	205	107	ND	ND	72%	40,577	ND	ND	ND
55	332	255	63	296	106	26	229	87%	ND	ND	ND	ND
150	761	382	261	594	172	108	274	ND	212,868	ND	ND	ND
177	755	396	280	454	159	150	246	87%	175,248	467*	31	8
337	1,642	902	626	601	139	492	410	ND	ND	496*	77	17
357	ND	ND	ND	ND	ND	ND	ND	ND	221,374	ND	ND	ND
370	ND	ND	ND	ND	ND	ND	ND	95	ND	ND	ND	ND
433	1,520	772	574	422	129	ND	ND	ND	ND	287*	78	28

ND, Not done.
*On intravenous immunoglobulin.

TABLE E3. WES read and base call statistics

Sample name	Total paired-end reads	Mapped reads (MAQ > 30)	Total bases called	On-target bases called (≥1X)	On-target bases called (≥30X)	Median depth of coverage
F1-A	66,429,212	54,732,674	86,149,939	51,034,733	40,186,431	74
F2-A	70,791,168	58,882,749	85,170,348	50,783,664	38,972,762	76
F2-F	96,606,359	61,096,692	84,959,171	50,635,756	38,335,215	77
F2-M	66,003,787	52,384,369	86,536,860	51,143,914	41,020,229	74
F2-U1	87,441,596	59,688,282	87,086,912	51,204,638	42,386,219	83
F2-U2	71,219,534	59,161,220	87,230,883	51,358,063	42,697,860	84
F3-A	75,264,785	57,315,943	87,183,415	51,335,129	41,999,740	79
F6-A	89,480,810	38,675,864	86,038,270	51,091,946	39,078,054	57
F6-F	122,885,291	90,721,645	88,560,143	51,565,697	46,623,537	134
F6-M	84,131,015	57,320,623	87,451,873	51,315,152	43,632,225	84
F6-U	110,171,535	84,544,225	87,964,382	51,377,214	45,774,189	121
F7-A	89,681,933	71,993,221	88,193,905	51,537,309	45,032,696	101
F7-F	92,230,748	87,930,551	88,517,319	51,593,234	46,795,800	124
F7-M	143,658,092	132,598,000	88,311,621	51,466,745	47,398,869	178
F7-U	99,370,206	91,683,239	88,717,675	51,620,982	47,367,218	131

TABLE E4. Mapping statistics of WES datasets

Sample name	No. of bases 1X	No. of bases 10X	No. of bases 20X	No. of bases 30X	No. of bases 40X	No. of bases 50X	No. of bases 60X	No. of bases 70X	No. of bases 80X	No. of bases 90X	No. of bases 100X	No. of bases >100X	Median depth of coverage	Mean depth of coverage
F1-A	51,034,733	47,276,848	43,751,442	40,186,431	36,601,574	33,115,120	29,827,580	26,761,614	23,947,568	21,392,696	19,087,205	18,869,677	74	100.08
F2-A	50,783,664	46,144,460	42,394,513	38,972,762	35,803,023	32,825,904	29,980,391	27,232,742	24,594,000	22,096,250	19,767,895	19,544,897	76	97.94
F2-F	50,635,756	45,741,140	41,804,034	38,335,215	35,231,673	32,443,474	29,830,957	27,357,690	24,983,644	22,720,464	20,578,379	20,371,816	77	100.11
F2-M	51,143,914	47,693,293	44,401,958	41,020,229	37,507,446	33,963,377	30,467,477	27,120,083	23,993,131	21,116,559	18,531,620	18,289,378	74	94.09
F2-U1	51,204,638	48,234,355	45,352,925	42,386,219	39,249,240	36,023,452	32,788,252	29,629,458	26,618,216	23,810,993	21,225,374	20,979,407	83	104.62
F2-U2	51,358,063	48,412,015	45,584,625	42,697,860	39,649,372	36,475,643	33,233,780	30,024,652	26,929,386	24,022,781	21,330,874	21,075,057	84	104.51
F3-A	51,335,129	48,164,401	45,119,768	41,999,740	38,708,938	35,326,436	31,929,847	28,632,366	25,496,204	22,606,444	19,989,228	19,743,008	79	102.06
F4-A	51,091,946	47,418,046	43,534,874	39,078,054	34,183,024	29,193,506	24,466,217	20,272,696	16,703,388	13,745,017	11,319,494	11,102,602	57	70.31
F4-F	51,565,697	49,902,806	48,226,973	46,623,537	44,993,717	43,271,901	41,435,143	39,494,097	37,434,856	35,294,266	33,098,895	32,877,939	134	159.65
F4-M	51,315,152	48,840,848	46,318,492	43,632,225	40,621,952	37,319,240	33,826,017	30,298,817	26,885,512	23,681,752	20,755,427	20,480,270	84	101.87
F4-U	51,377,214	49,420,379	47,549,375	45,774,189	43,925,953	41,945,934	39,838,754	37,602,675	35,282,753	32,919,494	30,554,552	30,319,768	121	149.47
F5-A	51,537,309	49,447,243	47,244,731	45,032,696	42,648,888	40,068,772	37,325,973	34,495,303	31,630,279	28,808,907	26,111,213	25,849,141	101	126.94
F5-F	51,593,234	50,021,717	48,389,626	46,795,800	45,116,446	43,266,875	41,200,668	38,943,191	36,543,448	34,058,521	31,547,099	31,298,637	124	157.65
F5-M	51,466,745	50,013,225	48,640,258	47,398,869	46,199,070	44,981,218	43,716,616	42,383,771	40,998,154	39,548,180	38,030,088	37,875,686	178	225.17
F5-U	51,620,982	50,284,375	48,824,827	47,367,218	45,838,889	44,152,519	42,266,310	40,187,790	37,940,200	35,563,636	33,140,286	32,897,507	131	161.93

TABLE E5. Statistics of variants identified with WES in the 5 core families

Families	Samples	Total variant count	Total variant count/family	Total variant count/sample	SNV/sample	Indel/sample
F1	F1-A	109,877	48,899	48,899	44,216	4,683
F2	F2-A		70,163	47,936	43,107	4,829
	F2-F			47,744	42,982	4,762
	F2-M			49,322	44,630	4,692
	F2-U1			49,845	45,167	4,678
	F2-U2			49,474	44,809	4,665
F3	F3-A		48,357	48,357	43,635	4,722
F4	F4-A		68,710	48,848	44,127	4,721
	F4-F			49,172	44,480	4,692
	F4-M			49,693	44,973	4,720
	F4-U			50,146	45,296	4,850
F5	F5-A		68,407	49,161	44,488	4,673
	F5-F			49,502	44,838	4,664
	F5-M			49,746	45,101	4,645
	F5-U			49,928	45,173	4,755

TABLE E6. Statistics of variants following different possible modes of inheritance

Category	Autosomal recessive	X-linked recessive	Pseudoautosomal	Germline *de novo*	Compound heterozygous
All variants following mode of inheritance					
Family 1	17,395	343	21	/	/
Family 2	995	87	2	665	67
Family 3	18,563	776	12	/	/
Family 6	1,650	52	0	752	32
Family 7	1,516	65	0	579	49
Potentially damaging rare variants					
Family 1	130	5	0	/	/
SNV	81	1	0	/	/
Indel	49	4	0	/	/
Family 2	14	5	0	96	34
SNV	8	5	0	81	/
Indel	6	0	0	15	/
Family 3	138	48	0	/	/
SNV	80	40	0	/	/
Indel	58	8	0	/	/
Family 6	13	3	0	56	17
SNV	9	3	0	49	/
Indel	4	0	0	7	/
Family 7	15	8	0	25	23
SNV	14	8	0	24	/
Indel	1	0	0	1	/

Screening filters: not-in-segment duplication regions, nonsynonymous/stop-gain/stop-loss, and 1000 Genomes Project minor allele frequency of 0.05 or less. The damaging nature of the variants were also evaluated with SIFT (<0.05), PolyPhen-2 (>0.85), and SIFT Indel predictions (Cause NMD = yes), although these were not initially used as strict filters.